

BACHELOR

FTIR reflection spectroscopy of hydrogenated silicon amorphous films

Kalcik, S.

Award date:
2011

[Link to publication](#)

Disclaimer

This document contains a student thesis (bachelor's or master's), as authored by a student at Eindhoven University of Technology. Student theses are made available in the TU/e repository upon obtaining the required degree. The grade received is not published on the document as presented in the repository. The required complexity or quality of research of student theses may vary by program, and the required minimum study period may vary in duration.

General rights

Copyright and moral rights for the publications made accessible in the public portal are retained by the authors and/or other copyright owners and it is a condition of accessing publications that users recognise and abide by the legal requirements associated with these rights.

- Users may download and print one copy of any publication from the public portal for the purpose of private study or research.
- You may not further distribute the material or use it for any profit-making activity or commercial gain

FTIR reflection spectroscopy of hydrogenated silicon amorphous films

Kalcik, S.

July 11, 2011

Abstract

The reflection and transmission spectra of crystalline silicon and glass substrates with hydrogenated amorphous silicon films, deposited by the expanding thermal plasma method were measured. Optical constants and absorbance spectra were calculated using Kramers-Kronig relations between the real and imaginary parts of the complex refractive index. The results show that specular reflection Fourier transform infrared measurements are suitable to evaluate thin films on silicon substrates, while these measurements aren't as suitable to evaluate thin films on glass substrates. Kramers-Kronig analysis is needed to get a clear absorbance spectrum from reflection Fourier transform infrared measurements. An increase in film thickness provide stronger reflection signals. However, the reflection signals are too weak for proper characterization of hydrogenated amorphous silicon films on glass substrates due to the high absorption of infrared light by glass.

Contents

1	Introduction	3
2	Theory	5
2.1	Theoretical considerations	5
2.2	Kramers Kronig transform	5
2.3	Vibrational modes	7
3	Experiment	9
3.1	Deposition setup	9
3.2	Film analysis	11
4	Results & Discussion	12
4.1	K-K analysis	12
4.2	Influence of film thickness	14
4.3	Comparison of spectra	18
5	Conclusion	19

Chapter 1

Introduction

A solar cell is a photovoltaic (PV) device that converts sunlight directly into electricity. This device provides a clean and decentralized renewable energy source. The present market is dominated by Si wafer based solar cell technology. In the year 2009 the PV market amounted for 81% of the overall market [1]. Polycrystalline silicon (poly-Si) thin-film solar cells ($<10 \mu\text{m}$), with low cost substrates such as glass, can offer high cell efficiencies combined with reduced production cost and material consumption compared to Si wafer based solar cells [2]. In the recent years noticeable progress has been made with low cost poly-Si thin film solar cells. First solar modules based on poly-Si on glass substrate have entered mass production in 2006 [3].

Recently, poly-Si layers ($1 \mu\text{m}$ thick) have been developed with grains extending through the layer thickness upon solid-phase crystallization (SPC) of high grow rate ($> 8 \text{ nm/s}$) expanding thermal plasma (ETP) deposited hydrogenated amorphous silicon (a-Si:H) films [4]. During solid-phase crystallization a-Si:H films undergo a phase transformation and as a result fully (poly-)crystallized films are obtained. The effect of the amorphous silicon microstructure on the grain size of SPC poly-Si has been investigated recently [5]. In that study a-Si:H films were deposited at different microstructural parameter values R^* (which represent the distribution of Si-H_x bonds in amorphous silicon), at a constant hydrogen content. The following was concluded: An increase in amorphous film structural disorder (i.e. an increase in R^*), leads to the development of relatively large grain sizes (700-1100 nm). For lower values of the microstructure parameter the grain size ranges between 100 and 450 nm. The results from this study show that the microstructural parameter has a key role in controlling the grain size of the poly-Si and thus the performance of poly-Si solar cells. To evaluate the quality of a-Si:H thin films it is therefore necessary to determine the microstructure factor R^* . R^* can be obtained from Fourier transform infrared spectroscopy (FTIR) (the method is described in more detail in Chap. 2.3).

FTIR is a useful technique for thin film measurements. Due to the high absorption of infrared light by most materials [6], including oxide glasses, the penetration depth can be less than $0.1 \mu\text{m}$ in the wave number region $400\text{-}1500 \text{ cm}^{-1}$. Consequently FTIR spectroscopy is only sensitive to the composition of a thin surface layer and is useful for thin film analysis (such as a-Si:H thin films on glass substrates). Due to the transparency of silicon

substrates to infrared radiation, the technique is also useful for the quality evaluation of thin films such as a-Si:H deposited on crystalline silicon substrates.

In conventional setups a-Si:H films are deposited on silicon substrates and absorption spectra are obtained by transmission FTIR measurements. Since glass absorbs infrared light, the conventional setup for FTIR measurements can't be used. Instead, reflection FTIR measurements need to be considered. Not many papers have discussed thin films on glass substrates due to this complication [7]. However, the use of reflection FTIR measurements to evaluate films on silicon substrate has been examined before [7, 8]. In order to examine whether reflection FTIR measurements can be used as a common tool to evaluate thin films on glass substrates. This study intends to develop a basic understanding to use this technique to identify vibrational modes from the film and the influence of the substrate from experimental analysis and fundamental optics.

In the present report, the optical constants of a-Si:H films on glass and crystalline silicon substrates are calculated in the $370\text{-}7000\text{ cm}^{-1}$ region using K-K relations. In addition the relationship between the film thickness and the relative change of the reflectivity is investigated. For this purpose thickness series of a-Si:H films with thickness varying from 50 nm to 10 μm were deposited and the transmission and reflection FTIR spectra were compared. The structure is the following:

Chapter 2 presents fundamental knowledge about the Kramers Kronig transform. In addition an overview of the vibrational modes of an a-Si:H film is given, which will be used as a standard to compare reflection and transmission data.

Chapter 3 responds to the deposition of the a-Si:H thin films and characterization. Experimental setups used for the expanding thermal plasma deposition (ETP) of a-Si:H films and FTIR analysis are described in detail.

Chapter 4 reports the results from FTIR analysis and is devoted to the discussion of these results before finally concluding in **Chapter 5**.

Chapter 2

Theory

2.1 Theoretical considerations

As mentioned before due to the complications of the thin films on glass to IR reflection, reflection FTIR measurements need to be used instead of transmission measurements. Other complications arise when measuring reflection spectra, which will now be discussed.

In reflection spectroscopy an absorption band is associated with the variation of extinction coefficient in a material. An increase in the extinction coefficient causes energy to be removed from the reflected radiation. The resulting spectrum looks like a transmission spectrum, where absorption bands can be seen as bands of reduced energy. In transmission spectroscopy the absorption band is associated with the variation of extinction coefficient in a material. There is a slight dependence of the position of the transmittance minimum on the index of refraction [9]. To calculate the significance of such an effect on a reflection spectrum Kramers Kronig (K-K) analysis is required.

2.2 Kramers Kronig transform

Determination of the complex refractive index constants, the complex dielectric constant, the absorption spectrum or the phase change of the IR beam (due to reflection from the sample) and the reflectance spectrum can be accomplished by K-K analysis. Causality restricts both the time-domain and frequency-domain responses of a system. The real and imaginary parts of the frequency-domain response are related by the K-K relations. A proper K-K analysis requires the following conditions:

- The sample has to consist of a pure and homogeneous material (i.e. the sample may not consist out of mixtures, layered systems nor powders [10]).
- The beam has to be measured in specular reflection at nearly normal incidence.
- The sample must be thick enough to ensure that no light returns from the inner sample to the sample surface. Multiple reflections and interferences have to be avoided.

Roughening the backside of the sample prevents possible reflection if the sample is not thick enough to absorb all radiation [7].

- Also for K-K analysis of a reflection spectrum, a large part of the spectrum has to be measured and any unmeasured parts must be approximated with some adequate function [11].

Providing that the reflection spectrum $R(\omega)$ has been measured at near normal incidence, the mathematical form of the K-K expression relating the real and imaginary parts of the complex reflectivity $\hat{r} = re^{i\varphi}$ is

$$\varphi(\omega) = \frac{\omega}{\phi} \int \frac{\ln R(\omega') - \ln R(\omega)}{\omega^2 - \omega'^2} d\omega'. \quad (2.1)$$

Where $\omega = 2\phi\nu$ is the angular frequency and $\varphi(\omega)$ is the phase change of the infrared beam due to reflection. With the knowledge of both $R(\omega)$ and $\varphi(\omega)$, the real, n , and imaginary, k , part of the complex index of refraction may be calculated using the Fresnel equations [12]:

$$n(\omega) = \frac{1 - R(\omega)}{1 + R(\omega) - 2\sqrt{R(\omega)\cos\varphi(\omega)}} \quad (2.2)$$

$$k(\omega) = \frac{2\sqrt{R(\omega)\sin\varphi(\omega)}}{1 + R(\omega) - 2\sqrt{R(\omega)\cos\varphi(\omega)}} \quad (2.3)$$

The relation between the constants n , k , \hat{r} and R is as following:

$$R(\omega) = |\hat{r}|^2 = \frac{(n(\omega) - 1)^2 + k(\omega)^2}{(n(\omega) + 1)^2 + k(\omega)^2}. \quad (2.4)$$

It should be noted that in equation (2.4) the refractive index and absorption coefficient of air, respectively 1 and 0, are implemented. The complex dielectric constant, $\varepsilon_r = \varepsilon_1 - i\varepsilon_2$, and the complex index of refraction are interrelated:

$$\varepsilon_1 = n^2(\omega) - k^2(\omega) \quad (2.5)$$

$$\varepsilon_2 = 2n(\omega)k(\omega) \quad (2.6)$$

Also the absorbance, $A(\omega)$, can be calculated directly from the reflection spectrum $R(\omega)$ by:

$$A(\omega) = -\log_{10}(1 - R(\omega)). \quad (2.7)$$

In principle the K-K relations enable to determine all important optical constants from a single sample reflection spectrum. As mentioned in the previous section the film has to be thick enough to ensure a good reflection signal. A recent study has shown that the reflection signal increases linearly with the film thickness [13]. Another study of IR spectra of Plasma-enhanced chemical vapor deposition (PECVD) thin films on glass substrates has shown that due to the value of the refractive index of glass, the reflective signal is weak (approximately a factor 1000 smaller) for any system using a glass substrate compared to a system using a silicon substrate [7]. Conclusively, from a fundamental optical point of view K-K analysis of thin films on glass substrates may be problematic due to a weak reflection signal.

2.3 Vibrational modes

It is important to have an effective method for determining the composition and quality of a film. A convenient non-destructive tool for this purpose is to measure the infrared spectrum of a-Si:H thin films using a FTIR spectrometer. Quantitative analysis of various absorption strengths in such IR spectra allow proportionality constants to be determined for specific vibrational modes [14]. A typical transmission FTIR spectrum of a-Si:H is displayed in Fig.2.1.

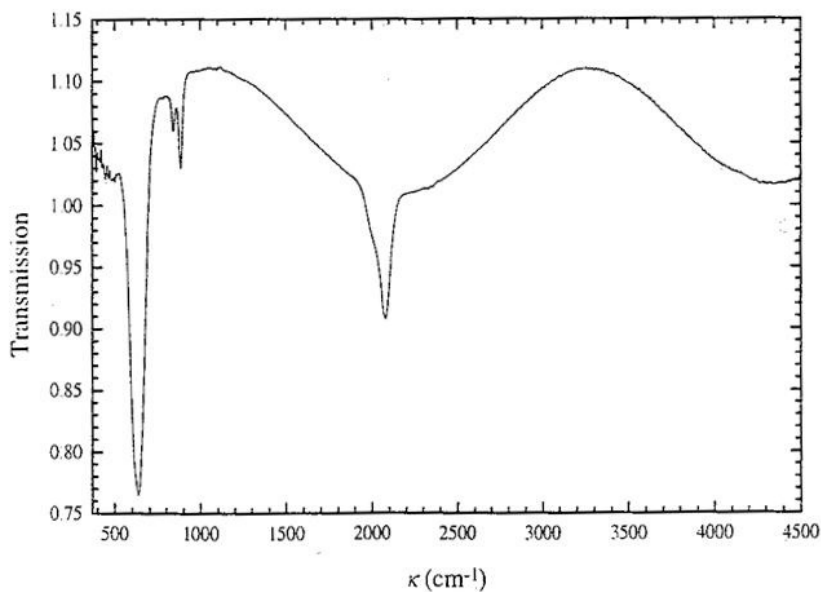


Figure 2.1: An example of a FTIR spectrum of an a-Si:H thin film displaying the vibrational modes [15].

The vibrational modes corresponding to the absorption peaks in Fig. 2.1 are tabulated in Table 2.1. An overview of the absorption peaks and the corresponding vibrational modes is given, because these will be used as a standard to compare transmission and reflection spectra and to determine whether reflection FTIR measurements can be used to characterize thin films on glass substrates.

Table 2.1: Vibrational modes of an a-Si:H film [15].

Wavenumber [cm^{-1}]	Vibrational modes
~ 640	Si-H _x wagging
~ 845	(Si-H ₂) _n bending
~ 880	Si-H ₂ bending
$\sim 1980 - 2030$	LSM:Si-H stretching
$\sim 2060 - 2120$	HSM:stretching Si-H on the surface of nano-sized voids, Si-H ₂ stretching

The quality of the a-Si:H film depends on the grain size of poly-Si. As mentioned in Chap. 1 R^* has a key role in controlling the grain size of poly-Si and is defined as following [16]:

$$R^* = \frac{I_{HSM}}{I_{LSM} + I_{HSM}}. \quad (2.8)$$

I_{HSM} and I_{LSM} are the integrated absorption intensities of respectively LSM stretching ($1980-2030 \text{ cm}^{-1}$) and HSM stretching ($2060-2120 \text{ cm}^{-1}$). Integrated absorption intensities can be determined from FTIR measurements.

Chapter 3

Experiment

The following chapter describes the deposition method of a-Si:H films onto glass and silicon substrates. Furthermore the method of film analysis is described.

3.1 Deposition setup

The expanding thermal plasma (ETP) is a remote plasma deposition technique, developed at the Eindhoven University of Technology [17], which allows deposition of good quality films at grow rates ranging from 0.2-60 nm/s [18, 19]. The main advantage of the ETP method is the high deposition rate that can be obtained for different materials.

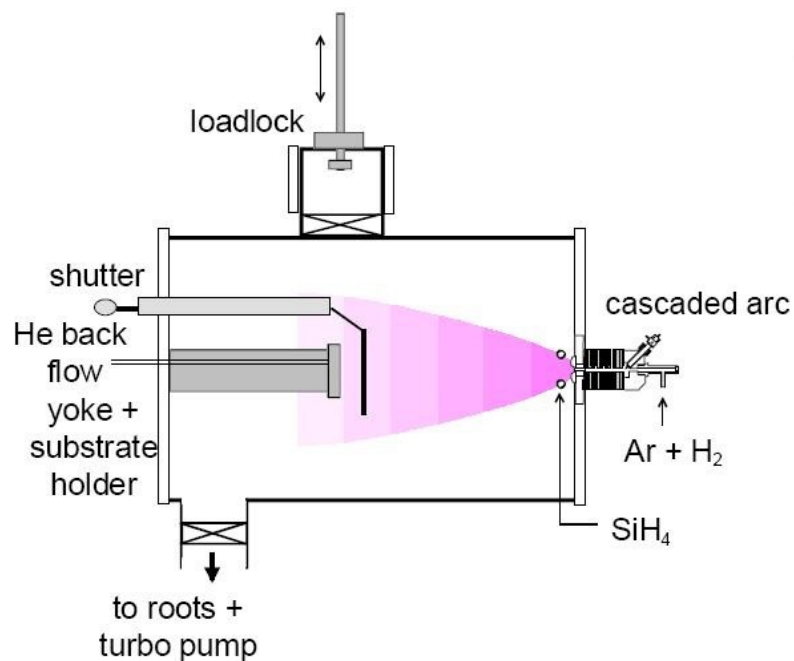


Figure 3.1: The expanding thermal plasma setup for a-Si:H deposition.

The deposition setup depicted in Fig. 3.1 consists of a low-pressure deposition chamber and a high-pressure plasma source. The cascaded arc serves as the plasma source (see Fig. 3.1) and is used to create reactive species for the dissociation of the precursor gas (SiH_4). In the vacuum-sealed cascaded arc a dc discharge in a non-depositing gas (Ar or Ar- H_2 mixture for a-Si:H) is sustained in the plasma channel between three cathodes and a grounded anode. The electrically insulated cascaded plates lead to a gradual potential drop. A dc power supply controls the discharge in the cascaded arc and the power dissipated is typically within 2-5 kW. The cathodes, plates and anode in the arc are all water cooled. The plasma in the arc is thermal with an electron density of 10^{22} m^{-3} and an electron temperature of 1 eV [17]. Because the deposition setup is operated on high flows (tens of sccs/several slm^1) of non-depositing gases, this leads to pressures of 0.2-0.6 bar when the plasma is ignited. The plasma expands from the cascade arc source through a nozzle and expands freely into the low-pressure (typically 0.1-0.3 mbar) deposition chamber. The plasma expands supersonically due to the large difference in the pressure between the arc and the chamber. It then creates a shockwave a few centimeters from the arc outlet, after which the plasma expands subsonically towards the substrate. The electron temperature is reduced to 0.1-0.3 eV in the supersonic expansion. The electron density reduces to 10^{17} - 10^{19} m^{-3} . The distance between the arc outlet and the precursor gas (SiH_4) injection ring is 5 cm, and the distance between the arc outlet and the yoke with substrate holder is 35 cm. Deposition can subsequently take place by the growth precursors at a temperature-controlled yoke with substrate holder. The substrates are protected from the plasma during plasma ignition by a shutter and are temperature controlled (100 - 500 °C) by a helium back flow. A loadlock chamber with a magnetic transfer arm is used to position the substrates into the system without the necessity of venting it.

Table 3.1: Experimental conditions used for a-Si:H film deposition.

Deposition Parameter	Value
Arc Current [A]	45
Ar Flow [sccm]	55
H_2 Flow [sccm]	10
SiH_4 Flow [sccm]	10
He Back Flow [sccm]	1
p_{reactor} [mbar]	0.165
p_{arc} [mbar]	353
$T_{\text{substrate}}$ [°C]	400

Depositions of a-Si:H were made on c-Si (crystalline silicon) and glass substrates. The typical experimental conditions are given in Table 3.1. The substrate temperature was set to 400 °C during all depositions. The working pressure was set to 0.165 mbar in the

¹sccs or 1 standard cubic centimeter per second = 1 cm^3 gas at 273 K and 1 atm. per second. 1 slm or 1 standard liter per minute = 16.7 sccs.

low-pressure chamber and the pressure at the high pressure source is 353 mbar during all depositions.

3.2 Film analysis

The a-Si:H films deposited using the ETP deposition method were analyzed using FTIR spectroscopy. Thin film's transmission and reflection spectra on both silicon and on glass substrates were taken.

The spectra were recorded on a Bruker Tensor 27 FTIR interferometer detector. The transmission measurements were conducted using a standard setup.

Reflection spectra were obtained using a specular reflectance accessory, which enables spectra acquisition at near-normal incidence. Incident and detection angles of the infrared light were set to 12° . A mirror was used as the reference for the samples. For the reflection spectra of thin films on a silicon substrate, silicon was also used as a reference. However, no differences has been found between reflection spectra with a mirror or the silicon sample as the reference.

All spectra were recorded with a resolution of 4 cm^{-1} taking 200 sample scans. The wavenumber accuracy is better than $\pm 1\text{ cm}^{-1}$. OPUS (OPTical User Software) [20] software package was used for spectra manipulations, including K-K transformations, and acquisitions.

Because the influence of the substrate is significant on the reflection measurements, thin films with varying thicknesses from 50 nm to $10\ \mu\text{m}$ have been deposited on top of both glass and silicon substrates using the ETP setup. The reflection spectra and both the absorption spectra and the complex refractive index, obtained by K-K transformation, were evaluated to reduce the impact from the substrate and to examine the influence of the film thickness on the peak's intensities and positions.

Chapter 4

Results & Discussion

Transmission and reflection spectra of a-Si:H thin films deposited on silicon and glass substrates have been measured for the following film thicknesses (under the conditions in Table 3.1): 50, 150, 250, 500, 750, 1000, 2500, 5000 and 10.000 nm. Subsequently K-K transformations on the reflection spectra have been performed in order to extract the complex refractive index and absorption spectra.

4.1 K-K analysis

In Fig. 4.1 the reflection spectrum and the real and imaginary parts of the complex refractive index are displayed for a a-Si:H film of 1200 nm deposited on a silicon substrate. After K-K analysis it is clear from Fig. 4.1, that the reflection FTIR measurement consists out of mixed data, i.e. it contains both dispersion and absorbance of infrared light. This can be seen by the presence of dispersion in the refractive index, n , in the same wavelength regions where gaussian shaped absorption peaks are visible in the absorbance coefficient, k [21]. The occurrence of dispersion and absorbance indicates that absorption spectra from reflection FTIR measurements are different from a corresponding absorption spectrum obtained by a transmission experiment [22].

After K-K transform the absorption peaks are also somewhat shifted. The peak at $\sim 621 \text{ cm}^{-1}$ (corresponding to Si-H_x wagging) is shifted after K-K analysis to $\sim 660 \text{ cm}^{-1}$. The peak at $\sim 1973 \text{ cm}^{-1}$ (corresponding to LSM:Si-H stretching) is shifted to $\sim 2012 \text{ cm}^{-1}$. Calculations shown in [23] predict an increasing adsorption for a decreasing value of n if other parameters are held constant. Conclusively, due to the influence of n the absorption peaks in a reflection spectrum are shifted towards higher wavenumbers relative to the transmission spectrum.

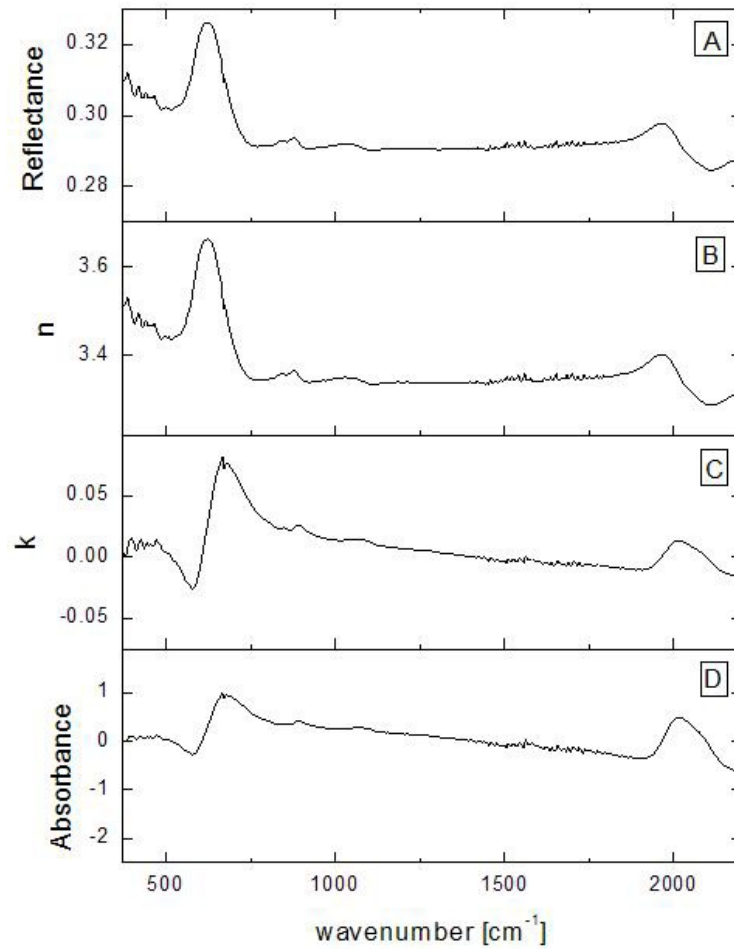


Figure 4.1: (A) reflection spectrum of an a-Si:H film of 1200 nm deposited on top of a silicon substrate. (B) real part of the complex refractive index. (C) imaginary part of the complex refractive index. (D) absorbance spectrum after K-K transform.

4.2 Influence of film thickness

The absorbance spectra (after K-K transformation of reflection FTIR measurements) obtained by reflection experiments of a-Si:H thin films with various thicknesses deposited on silicon substrates are given in Fig. 4.2. From Fig. 4.2 can be seen that the absorption peaks at $\sim 2000 \text{ cm}^{-1}$ increase with increasing film thickness. The same can be said for the peak at $\sim 640 \text{ cm}^{-1}$, only this peak is upside down with respect to normal absorption, as can easily be identified from a transmission spectrum from a silicon substrate (see Fig. 4.6). A previous study of reflective spectra of PECVD thin films on glass substrates[7] has also shown the same changes in peaks as mentioned above, though also a shift in the peak positions towards lower wavenumbers with increasing thickness was observed. In that study only a significant change in peak positions was observed in films thicker than $3 \mu\text{m}$. The noise present in the region $1300 - 1800 \text{ cm}^{-1}$ is caused by contamination due to water vapor.

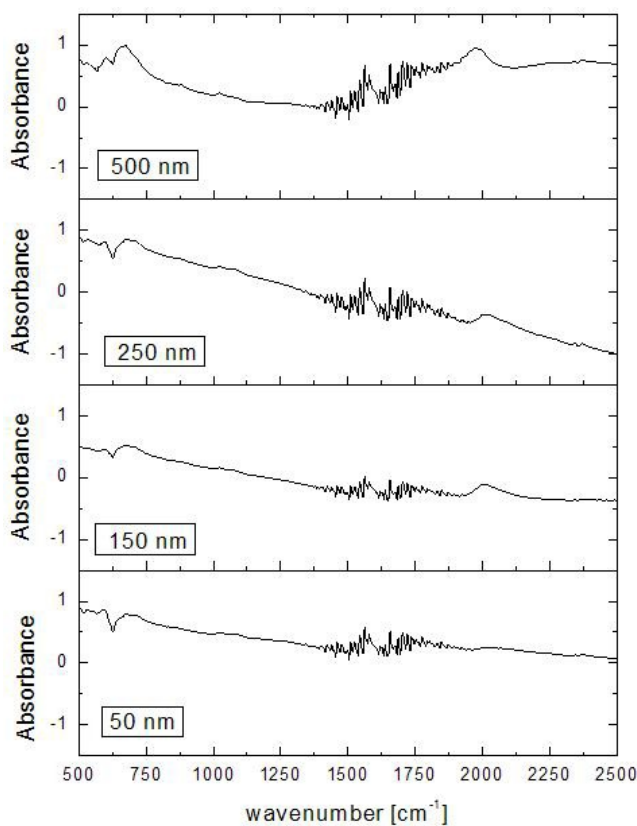


Figure 4.2: Absorbance spectra after (K-K transformation) of a-Si:H films deposited on silicon substrates with thicknesses of 50, 150, 250 and 500 nm.

Absorbance spectra (after K-K transformation of reflection FTIR measurements) of relative thicker films (i.e. $\geq 1 \mu\text{m}$) are given in Fig. 4.3. Due to the relative high film thickness an interference pattern of IR light is created. Light from the top of the film

surface and light from the interface between the film and substrate is in interference. This pattern can be seen as fringes. This complicates the detection of absorption peaks. The fringes caused by interference can be removed using a Fourier filtering procedure [24]. Although the fringes make it difficult to detect absorption peaks caused by vibrational modes, they can be used to determine the film thickness. An increase of the reflected signal is expected with an increase in film thickness. From Fig. 4.3 it is clear however, that an increase in film thickness doesn't make the absorption peaks (corresponding to the vibrational modes in Table 2.1) more visible. The lack of clearly visible absorption peaks can be explained by the increase of inhomogeneity of the a-Si:H films. Depositions of a-Si:H films on substrates with a thickness of several microns have thousands of monolayers. Therefore the homogeneity of the film decreases when the thickness a film is increased.

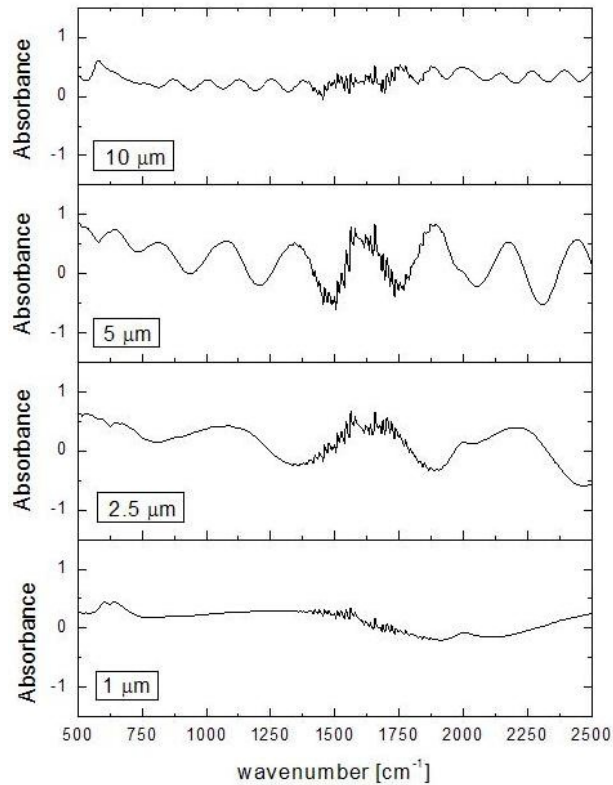


Figure 4.3: Absorbance spectra after (K-K transformation) of a-Si:H films deposited on top of silicon substrates with thicknesses of 1, 2.5, 5 and 10 μm .

The absorbance spectra (after K-K manipulation of reflection FTIR measurements), obtained by reflection experiments of a-Si:H thin films deposited on glass substrates, are given in Fig. 4.4.

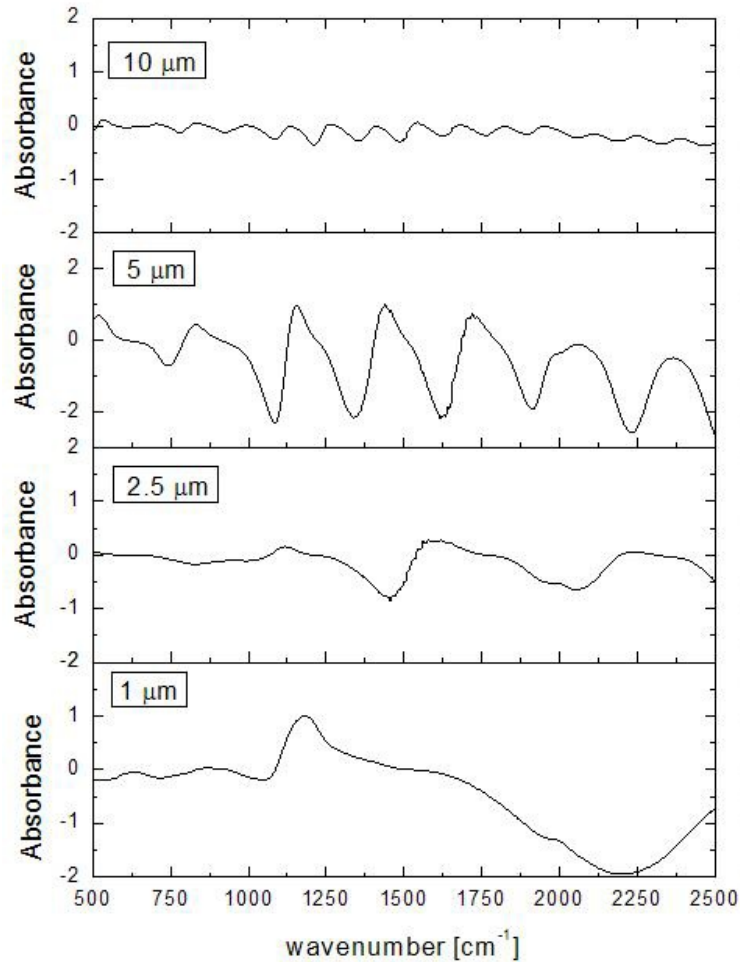


Figure 4.4: Absorbance spectra after (K-K transformation) of a-Si:H films deposited on top of glass substrates with thicknesses of 1, 2.5, 5 and 10 μm .

Fringes are visible from interference of infrared light due to the high thickness of the film (as was observed with the films on silicon substrates). Absorbance spectra of thinner films (i.e. $\leq 1 \mu\text{m}$) have also been measured but are not displayed. K-K transformation of these thinner films yielded nonphysical results for the complex refractive index and absorbance and were therefore omitted. This may indicate that the reflection signal from the thinner films is too weak. To make this assumption credible a reflection FTIR measurement has been taken of a $1 \mu\text{m}$ thick a-Si:H film deposited on a glass substrate and a layer of gold has been added between the film and substrate. The absorbance spectrum after K-K transformation is given in Fig. 4.5. In Fig. 4.5 the absorption peak at ~ 640 and 2100 cm^{-1} are visible. Again the peak at $\sim 640 \text{ cm}^{-1}$ is up side down with respect to normal

absorption. The noise present in the region $1300 - 1900 \text{ cm}^{-1}$ is caused by contamination due to water vapor. Conclusively, absorption peaks are only visible when a gold layer is deposited between the film and the glass substrate, which indicates that the reflected signal from the film on the glass substrate is too weak for proper K-K analysis.

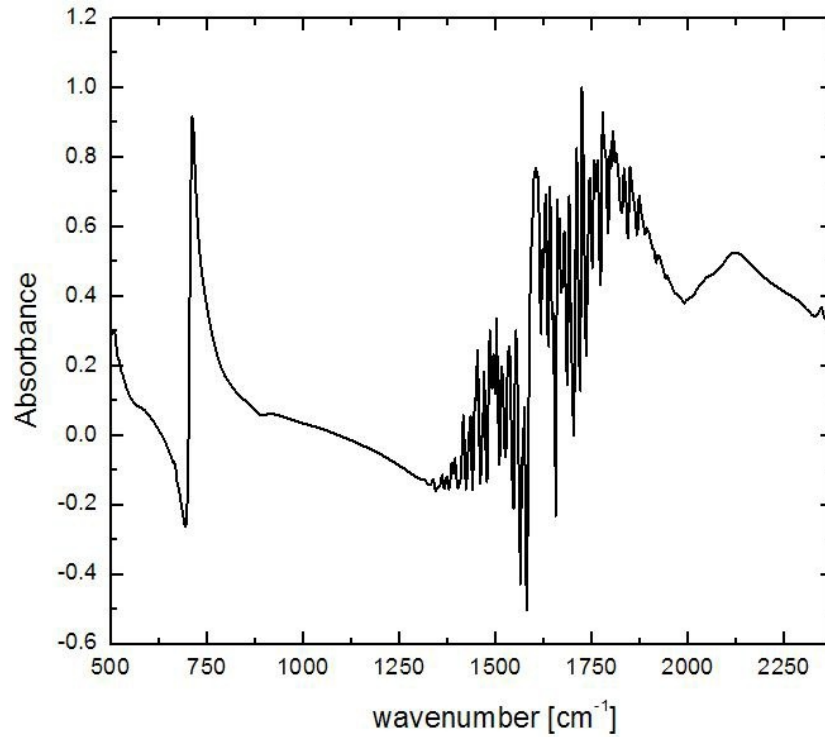


Figure 4.5: Absorbance spectrum after K-K transformation of $1 \mu\text{m}$ thick a-Si:H film deposited on top of a glass substrate with a layer of gold deposited between the film and substrate.

4.3 Comparison of spectra

The absorbance spectra from Figures 4.2, 4.3 and 4.4, obtained by reflection experiments, are compared with absorbance spectra obtained by a transmission experiment (given in Fig. 4.6). It is evident that the signal reflected from the film is weak in comparison to transmission. While the absorption peak at ~ 640 and 2000 cm^{-1} are clearly visible in the absorbance spectrum from Fig. 4.6 they are not as clearly visible for samples with the same film thickness in Figures 4.3 and 4.4. The difference between the absorbance spectra obtained by both transmission and reflection can be explained by the presence of scattering in the reflection mode. In transmission light passes through the film and substrate. There is no or little scattering. In reflectance, however, the photons are scattered. Due to this scattering weak features not normally seen in transmission are enhanced. In theory this should increase reflection FTIR measurements as a tool for characterization of films. But the signal from reflectance is too weak in practice, as demonstrated.

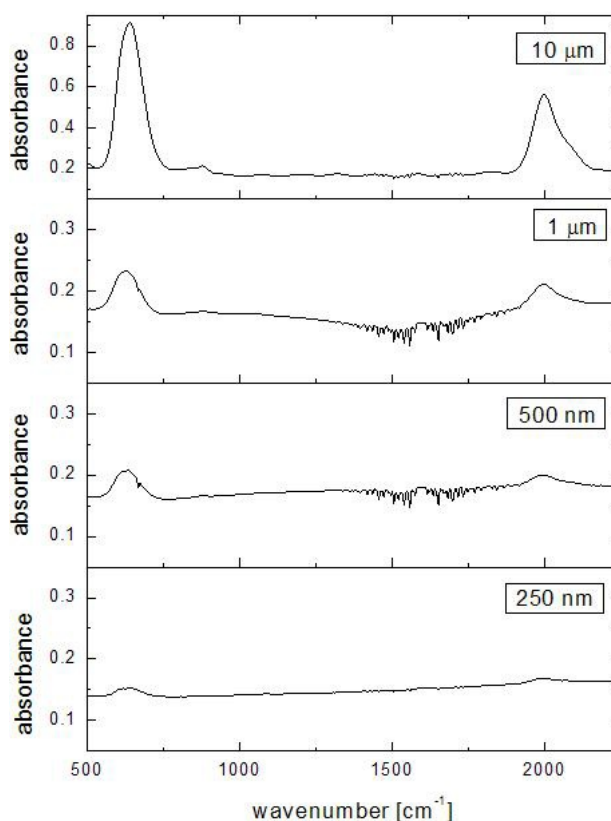


Figure 4.6: Absorbance spectra (obtained by a transmission experiment) of a-Si:H films deposited on top of a silicon substrate with thicknesses of 250 nm, 500 nm, 1 μm and 10 μm .

Chapter 5

Conclusion

In this report a novel approach for infrared reflection spectra of a-Si:H films on glass and silicon surfaces is introduced. The reflection spectra from a film thickness series ranging from 50 nm to 10 μm deposited on top of both silicon and glass were used as example to determine the absorbance spectra and the complex refractive index. The experimental results and results from fundamental optics reveal the following:

- Reflection spectra from glass substrates are much weaker than those from silicon substrates. This is caused by the difference of refractive index between the glass substrate and thin film, which is significantly smaller than silicon substrate to thin films[7].
- K - K analysis is needed to get a clear absorbance spectrum from reflection FTIR measurements, without a mixture of absorption and dispersion.
- Thicker films (with properties described in section Kramers Kronig transform of this report) provide stronger reflection signals, however, as demonstrated by the addition of a deposited layer of gold between the film and the substrate, the signals are too weak.
- Reflection FTIR measurements can provide information for the characterization of films, for silicon substrates. For the analysis of glass a stronger reflection signal is required.

Raman spectroscopy is suggested as an alternative method for the characterization of a-Si:H thin films. The advantage of Raman spectroscopy over FTIR spectroscopy is that there is no concern with sample thickness, size or shape. Furthermore background species, such as carbon dioxide and water vapor all have weak Raman spectra. Therefore background correction aren't necessary.

Bibliography

- [1] W.P. Hirshman and A. Schug. *Photon.* 4:38–65, 2010.
- [2] U. Schubert M. Keevers, T. Young and M. Green. In proceedings of the 22nd european photovoltaic solar energy conference. page 1783, Milan, Italy, 2007.
- [3] P. Basore. In proceedings of the 21st european photovoltaic solar energy conference. page 544, Dresden, Germany, 2006.
- [4] M. Creatore M.C.M. van de Sanden A. Illiberi, K. Sharma. *Matter let.* 63:1817, 2009.
- [5] A. Illiberi F. D. Tichelaar M. Creatore M.C.M. van de Sanden K. Sharma, A. Branca. *Advanced energy materials.* 1:401–406, 2011.
- [6] D.J. Masiello S.A. MacDonald, C.R. Schardt and J.H. Simmons. *Non-cryst. solids.* 275:72–82, 2000.
- [7] S. He. *Mat. res. soc. symp.* 508:127–132, 1998.
- [8] B.F. Hanyaloglu and E.S. Aydil. 44-th avs abstract. page 19.
- [9] R.R. Rahn R.G. Greenler and J.P. Schwartz. *Journal of catalysis.* 23:42–48, 1971.
- [10] V.M. Petrushevski V. Ivanovsky and B. Soptrajnov. *Vibrational spectroscopy.* 19:425–429, 1999.
- [11] A. Caron G. Andermann and D.A. Dows. *Optical society.* 55(10):1210–1212, 1965.
- [12] G.E. Tranter J.C. Lindon and J. Holmes. *Encyclopedia of Spectroscopy and Spectrometry.* Academic Press, 2000.
- [13] F. Hosoi M. Tamada, H. Koshikawa and T. Suwa. *Thin solid films.* 315:40–43, 1998.
- [14] D.M. Goldie and S.K. Persheyev. *Journal of mathematical sciences.* 41(16):5287–5291, 2006.
- [15] A.H.M. Smets and M.C.M. van de Sanden. *Physical review.* 76(7), 2007.
- [16] A.H. Mahan E. Bhattacharya. *Applied physics letters.* 52:1587, 1988.

-
- [17] M.D. Graaf J. Beulens and D. Schram. Plasma sources science and technology. 2:180–189, 1993.
- [18] L. Gabella F. van de Pas M. van de Sanden R. Severens, W. Kessels and D. Schram. Proceedings of 13th european photovoltaic solar energy conference and exhibition. 1997, PAGES = 1059.
- [19] J. Bastiaanssen W. Kessels L. van IJzenfoorn M. van de Sanden R. Severens, F. van de Pas and D. Schram. Proceedings of 14th european photovoltaic solar energy conference and exhibition. page 582.
- [20] Optical User Software for Tensor 27 FT-IR. *Version 4.2*. Bruker Optik, 2002.
- [21] K.E. Peiponen and E.M. Vartiainen. Physical review b. 44(15):8301–8303, 1991.
- [22] G.E. Tranter J.C. Lindon and J. Holmes. *Encyclopedia of Spectroscopy and Spectrometry*. Academic Press, 2000.
- [23] R.G. Greenler. Journal of catalysis. 44(310), 1966.
- [24] A.M.A. Pistorius and W.J. DeGrip. Vibrational spectroscopy. 36:89–95, 2004.